Review Article

BIOMEDICAL Journal of Scientific & Technical Research

ISSN: 2574 -1241

DOI: 10.26717/BJSTR.2023.48.007624

Very Accurate Temperature Control of Porcine Bones and Insulating Materials by CO_2 Laser: Experimental Data Supported by a Mathematical Model

Luc Lévesque*

Department of Physics and Space Science, Royal Military College of Canada, Canada

***Corresponding author:** Luc Lévesque, Department of Physics and Space Science, Royal Military College of Canada, Canada

ARTICLE INFO

Received: January 10, 2023

Published: January 25, 2023

Citation: Luc Lévesque. Very Accurate Temperature Control of Porcine Bones and Insulating Materials by CO2 Laser: Experimental Data Supported by a Mathematical Model. Biomed J Sci & Tech Res 48(2)-2023. BJSTR. MS.ID.007624.

ABSTRACT

In this report we are showing that temperature of porcine bone samples can be maintained to a constant value within the range 40ºC to 50ºC, which is essentially a range of interest for therapeutic treatment. For the afore-mentioned temperature range, it was also shown that a porcine bone sample could be kept at a given temperature within a fraction of a degree Celsius. This method relies on a real-time feedback computer-control between a non-contact sensor and a CO_2 laser operating at a repetition rate of 20 kHz. Results are shown for domesticated porcine bones that are strongly absorbing the CO_2 radiation at λ = 10.6 µm. Some results are also shown for Teflon and glass, which are insulators that are moderately absorbing at the afore-mentioned wavelength. A mathematical model is supporting the data that are presented in this report.

Keywords: COVID-19; Chemoprophylaxis; Aspirin; Atorvastatin; Arbs; Aceis; Hypertension; Diabetes Mellitus; Iran

Introduction

Careful temperature control within a few degrees Celsius is very important during therapeutic treatments of soft and hard tissues [1,2]. Accurate control of hard dental tissue surrounding a decayed region under laser ablation [3] within a tooth would also be very useful in order to avoid superheating or moderate heating during a selective process. Temperature control is very advantageous in methods such as laser photothermal ablation, which has been used to treat bone metastasis of breast cancer using multi-walled carbon nanotubes assisted with near-infrared at a wavelength of 808nm [4]. It can also be applied to low-level laser irradiation in knee osteoarthritis [5], where small temperature changes of 0.5°C favor significant improvement. It was also shown in soft tissue that the time of healing is greatly reduced as temperature increases by only 1°C [6]. Moderate power visible lasers were also shown to be successful in treating glaucoma [7,8]. Temperature control by feedback would also be applicable in laser-induced hyperthermia as the cellular response is highly dependent upon temperature [9]. Moreover, in tissue engineering, temperature control of the bone near the implant surface is very important as devitalization of the overlaying tissue may occur if the temperature exceeds 47°C [9-11].

In the above-mentioned medical treatments, temperature is not monitored in feedback when the laser beam is exposing tissue in real time. As the time-constant of non-contact IR thermal sensors is now comparable to the heat diffusion time and more adapted to computer-controlled applications, we are reporting a method that was developed to monitor and control temperature accurately on porcine bones, which can also be used in insulating materials. Methods to control temperature efficiently in liquids and porcine bones by CO_2 laser were shown to be adequate [12-14] with thermal sensors, but no feedback control was applied to regulate the lasing power during the procedures. A similar method to control temperature in porcine bones by CO_2 laser feedback was introduced earlier [15], but the mathematical and numerical simulations developed are confirmed by more data.

Methodology

A 10W CO_2 laser (Model#: 48-1KAL) from Synrad Inc. emitting at λ = 10.6 μm was used to investigate all the bone samples. The beam from the CO_2 laser aperture was reflected by a pair of mirrors that were introduced into a periscope assembly as shown in Figure 1a. The pair of mirrors was adjusted so that the beam propagates in a direction that is parallel to the plane of the optics table. Then the laser beam was collimated by two ZnSe lenses L_1 and L_2 of focal lengths f_1 (63.5mm) and f_2 (127mm), respectively. Within a region extending to about 1 meter from lens L_2 the laser beam spot size was measured by a knife-edge method to be roughly 3.5mm. Investigations on porcine bone or insulating materials samples were done in the far-field region in the presence of a third lens L_3 placed 25 cm behind L_2 as depicted in Figure 1. The focal length f_3 of lens L_3 was 127mm. For measurements in the far-field region, the bone or insulating material samples were positioned about 1.2m and 1.75m beyond lens L_3. The beam is strongly divergent in the far-field region beyond lens L_3. (Figure 1b) is showing how much the beam diverges after it is focused by lens L_3. The diameter of the CO_2 in Figure 1b was calculated by the ABCD matrices as described in a previous investigation on glass [16]. The advantage of investigating the specimens in the far-field is that a small portion of the large CO_2 beam (roughly 100mm) is exposing a piece of bone or insulating material that is 10 times smaller (10mm x 10mm). This method is making sure that the power density is uniform over each sample being investigated.

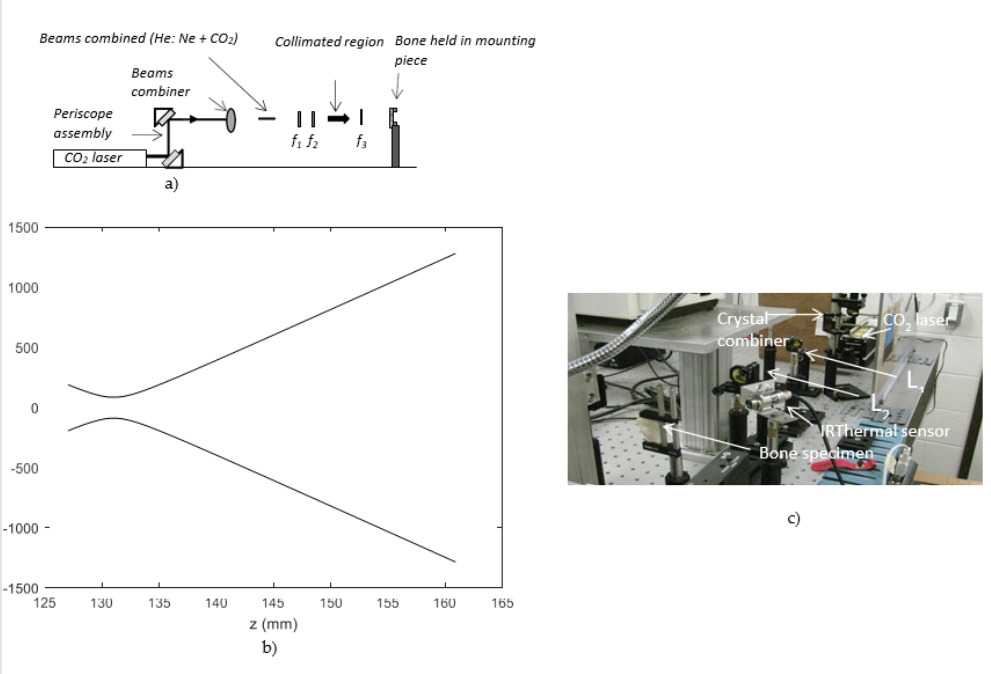

Figure 1:

a) Experimental set-up used to heat domesticated porcine bone samples (bone not shown).

b) Divergence of the CO_2 beam after the focal point from the values of f_1, f_2 and f_3 given in the text.

c) Experimental set-up showing the He: Ne laser redirected by the crystal combiner. Lenses L_1 and L_2 are also shown with the IR thermal sensor and the bone specimen inserted into a mounting piece. L_3 is not shown for the sake of clarity.

Another advantage is that a small increase in power translate into a small power density incremental amount, which is improving the resolution and reduce the variation of temperature around a desired value. This improvement in resolution will be shown in the experiment section. Just before the pair of lenses L_1 and L_2, a red beam of light from a He: Ne laser was aimed in a direction that is perpendicular to the CO_2 laser beam. This beam of red light was reflected on one face of a crystal combiner (c.f. (Figure1b)) and was then taking the same path as the transmitted CO_2 laser beam. The He: Ne laser beam was used as a safety precaution during the manipulations and was also used to identify the region that was irradiated on the porcine bone specimen before each trial. Note that the thermal sensor is not shown in Figure 1a. Porcine bones were chosen because laser ablation produced in the animal bones is very similar to findings in hard biological tissues such as human tooth [17]. Porcine bones were cut into thin pieces having thicknesses between 1.5 and 2mm. The bones were cleaned in a solution of hydrogen peroxide (3%) for an hour and then left to dry in a well ventilated area for a few days. With these bone thicknesses varying within 1.5 to 2mm, the time for each specimen to reach a steady state in temperature was minimized. The principle used to keep the temperature within a small temperature range is relying in the communication between the CO_2 laser source and the IR thermal sensor (Model: PMU201) from Calex Electronics Ltd, which is measuring the temperature from the radiative heat loss. When the laser irradiates the sample at a given power as shown in Figure 2a, the radiative heat loss from the sample surface is increasing

and the IR thermal sensor records the temperature. Let us say, that one wishes to keep the sample surface at a temperature of 100°C ±1°C. If temperature T is increasing and reaches a value greater than an upper limit, say 101°C, a command is sent to the laser to lower the power so the temperature can drop below 101ºC.

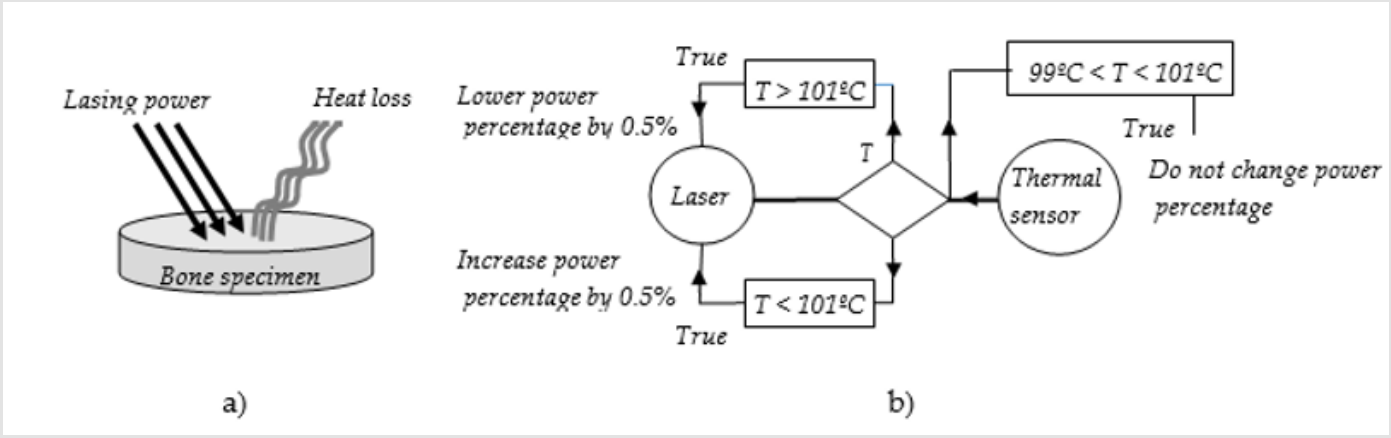

Figure 2:

a) Bone specimens being irradiated by a CO_2 laser source at λ= 10.6 μm

b) Flow chart of the main programming step performed during a data acquisition.

If temperature T is decreasing to a value lower than 99°C, a command is sent to the laser source to increase the power so the temperature can increase in order to keep the sample surface at 100°C within ±1°C. Figure 2b is showing a flow chart of the main steps performed during the data acquisition, when the sample surface is kept at 100°C within a margin of 1°C during a typical experimental trial. The temperature that was targeted in this example was 100°C ±1°C, but any desired temperatures within 40 to 100˚C were attempted in our investigations. During our investigations with porcine bones, the experimental set-up shown in Figure 1 was used to raise or lower the temperature of the specimens. When the CO_2 laser is irradiating the porcine bone specimens at a constant power without any correction of power to compensate for a temperature change (without feedback), it is not possible to keep the surface temperature constant with time. Within 40˚C and 100˚C, heat conduction and convective transfers are moderate, but sudden air draft can still cause variations in temperature. As a result, the surface temperature kept increasing slowly with time and takes a very long time to reach a temperature T, which varies at a slow rate and never reaches a steady value when no feedback correction is applied. It was found that temperature is rising much more quickly to the desired value when a feedback method is applied and the fluctuating temperature can be within a degree Celsius in some conditions. This behavior of the material temperature for the feedback method previously described will be explained in more details in the next sections.

Mathematical Modelling

As bones have high absorption at the CO_2 wavelength, only a very small layer confined near the bone surface will be heated. The thickness t of this layer confined near the surface is attenuating the laser beam irradiation by direct absorption according to Beer's law [18,19]. Therefore, in the case of a disk of material the laser irradiation will decay exponentially from the surface as:

$$I(z) = I_o \exp(-\alpha z) \quad (1)$$

where α is the absorption coefficient, Io is the laser irradiation at the material surface and $3a^{-1}$ is the distance from the surface. At a distance $d \approx 3\alpha^{-1}$ from the material surface, Eq. (1) predicts that the irradiation is roughly 5% of the initial value Io. As a result, in our investigations we may estimate the layer heated by the CO_2 laser as d ~$3a^{-1}$. Bone material consists of roughly 15% water, about 25% collagen and 60% hydroxyapatite and calcium phosphate [19,20]. According to values reported in the literature [20,21] from the relative abundance of the constituents of a bone and the absorption value for each of them, the averaged absorption coefficient α for bone is roughly 2500 cm^{-1}, which means d ~13 μm at $\lambda = 10.6\mu m$. The scattering coefficient reported in the literature for hard bones in the mid-infrared from 2 μm to 10.6 μm is on the order of 10 cm^{-1} [22,23] or is too small to be measured [24,25] at $\lambda = 10.6\mu m$. As the scattering coefficient reported for hard tissues is very small compared to the absorption coefficient α, the scattering loss is neglected in Eq. (1). The general heat conduction equation [26,27] will be applied to the material when the bone is being irradiated by the CO_2 laser and when the laser is momentarily turned off. The general heat conduction equation is:

$$\frac{\partial T(z,t)}{\partial t} = K\frac{\partial^2 T(z,t)}{\partial z^2} + \frac{Q(z,t)}{\rho c} \quad (2)$$

where $K = k/\rho c\left(cm^2 s^{-1}\right)$ is the thermal diffusivity, k is the thermal conductivity, ρ is the material density, c is the heat capacity, $Q(z,t)$ is a heat source term $\left(W/cm^3\right)$, and $\partial T/\partial t$ is the rate of change of the material's temperature. Before any laser pulses were applied, all the

bone specimens used in this investigation were in equilibrium with the laboratory temperature. When the laser is on, the irradiance at the air-bone interface (z=0) is taken into account. No chemicals generating heat such as exothermic reactions in the bone is being considered and as a result, the heat source term Q (z,t) will be assumed to be equal to zero. Therefore, when the specimens are being heated (c.f. Figure 2a), the problem is formulated as follows:

$$\frac{1}{K}\frac{\partial^2 T(z,t)}{\partial z^2}=\frac{\partial T(z,t)}{\partial t} \quad (3)$$

$$-k\frac{\partial T}{\partial z}=q_o-h(T-T_o), z=0, t>0 \quad (4)$$

$$T=T_0, z\to\infty, t>0 \quad (5)$$

$$T=T_0, z>0, t=0 \quad (6)$$

Laplace's transforms can be used to solve the partial differential Eq. (3) using the aforementioned boundary and initial conditions [28,29]. The solution is given by:

$$T(z,t)=T_o+\frac{q_o}{h}erfc\left(\frac{z}{\sqrt{4Kt}}\right)-\frac{q_o}{h}\exp\left(H^2Kt+Hz\right)erfc\left(H\sqrt{Kt}+\frac{z}{\sqrt{4Kt}}\right) \quad (7)$$

In Eq. (7), H= h/k and h is the heat transfer coefficient which has units of W/(cm^2.K). To is the temperature of the fluid or gas surrounding the material surface, which is air in our investigations. Because the laser power is modulated at frequencies of 20 kHz during our investigations, we also take into account the temperature drops when the laser is momentarily turned off. In the case of a sample cooling, the boundary condition prescribed by Eq. (4) is changed by setting q_o equal to zero. Also, as the sample surface rises its temperature to T_i as a result of heating (just before the power is turned off), the initial condition in equation 6 is changed to T (0,0) = T_i. The solution in the cooling cycle portion is given by:

$$T(z,t)=T_i+(T_i-T_o)\left[erfc\left(\frac{z}{\sqrt{4Kt}}\right)-\exp\left(H^2Kt+Hz\right)erfc\left(H\sqrt{Kt}+\frac{z}{\sqrt{4Kt}}\right)\right] \quad (8)$$

During our tests the increase in temperature is significant when the laser is turned on compared to the drop in temperature when the laser is momentarily turned off. Figure 3a is showing a simulation using Eq. (7) and (8) of the temperature change at z= 3.5 μm below the bone sample surface for the typical CO_2 laser modulation cycle shown in Figure 3b. Note that the change in temperature in Figure 4a is very sharp during the first 10 μs of the laser power cycle lasting 200 μs. The change in temperature during the time the laser power is turned off (190 μs) is hardly noticeable and the change in temperature is essentially looking like a staircase profile as shown in Figure 4a. During the first 10 μs of the modulation cycle (not on scale) shown in Figure 4b, the power delivered by the CO_2 is roughly 15W. For this portion of the cycle when the power is on, Eq. (7) was used. During the remaining part of the cycle, that is 190 μs, the power is turned off momentarily and Eq. (8) was used to calculate the temperature shown in Figure 4a. This method was used in our investigation to ramp the temperature to a desired value. Temperature control on porcine bones were obtained at 5 kHz and 20 kHz of frequency modulations. In the case of a 5kHz modulation, the material is heated for 10μs and the power drops to zero for 190 μs as shown in Figure 4b at 5% duty cycle. As the porcine bone absorb very much at $\lambda=10\mu m$, temperature is expected to fluctuate around the desired temperature. In the case of a feedback control at a frequency modulation of 20kHz at a duty cycle of 5%, the laser is on for only 2.5 μs and then it is turned off for 47.5 μs during the total period (repetition time) of 50 μs. As the temperature is not decreasing much during the cooling period when the laser is off (c.f. Figure 4a), the fluctuation in temperature around the desired T should be much less.

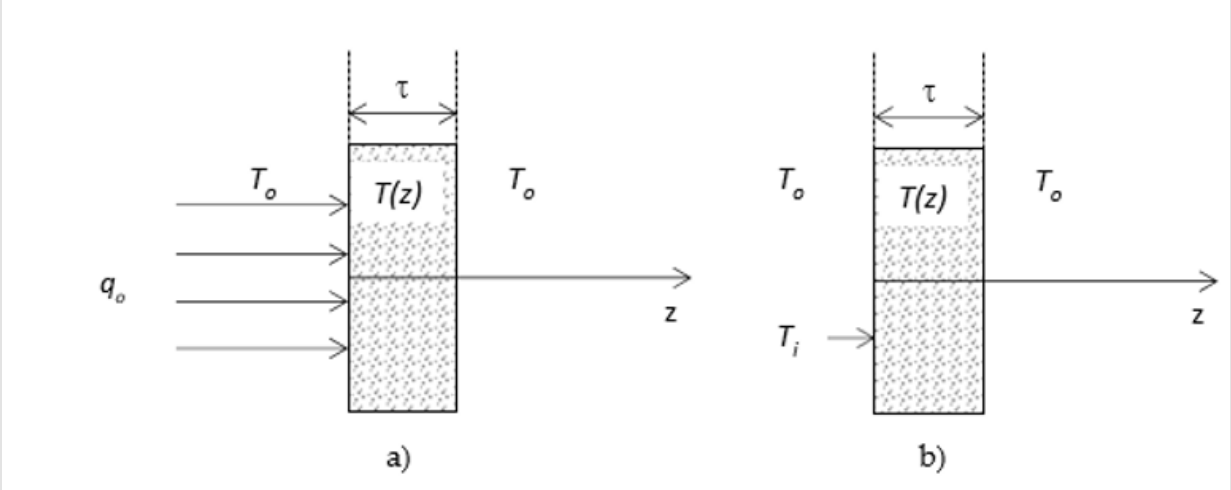

Figure 3: Bone specimen approximated by a slab for a thickness τ >> δ.

a) For a bone being irradiated at a power density qo

b) For a bone reaching a surface temperature Ti and the laser is suddenly turned off (qo =0). The bone is surrounded by the air at a temperature To.

 DOI: 10.26717/BJSTR.2023.48.007624

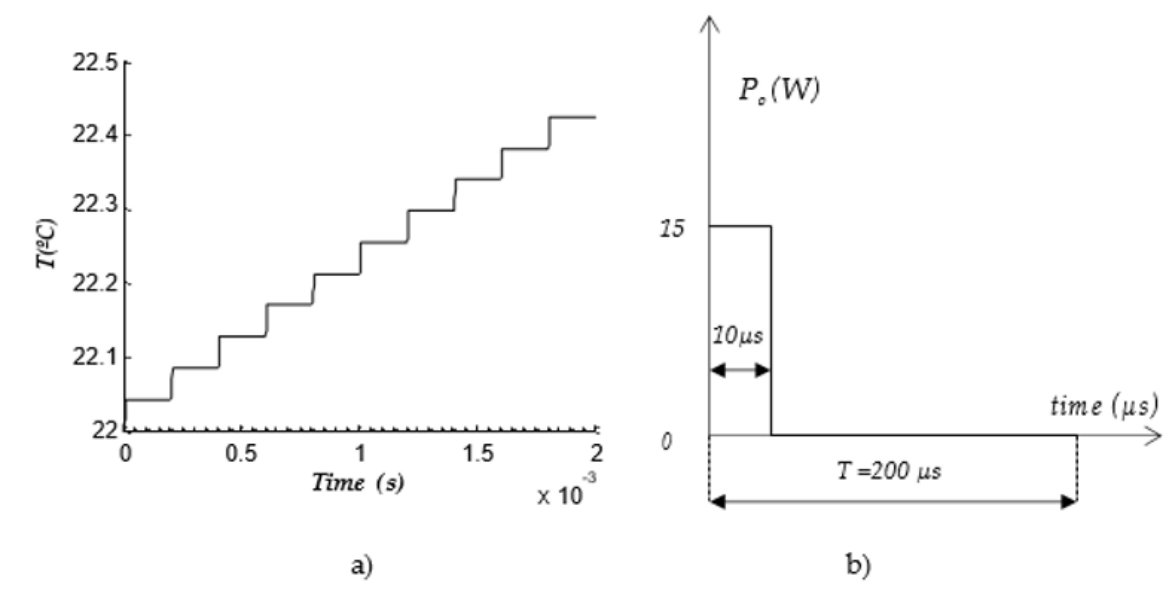

Figure 4:

a) Temperature change in a bone sample using equations 7 and 8. In this theoretical prediction the following data were used: To = 22ºC, qo = 1.2 x 106 W/m², ρ = 1180 kg/m3, k = 0.31/m. ºC, c = 2274 J/kgº C, h = 10W/m2 and z = 3.5 µm.

b) The repetition time of the modulation cycle (T = 200µs) for a duty cycle of 5% that was used for the theoretical prediction. For the CO_2 laser operating at a duty cycle of 5%, the laser power is on and delivers 15W for 10 µs and then is turned off momentarily for 190 µs. Note that the average power over the complete cycle is 5 percent of 15W, that is 0.75W.

Experiment

The CO_2 beam starts diverging after it is focused at a distance of 130 mm from lens L_3 (c.f. Figure 1b). This is so as the radius of a Gaussian beam (at $1/e^2$ points) is increasing with the propagation distance after it is being focused. This means that a change of 0.5% in the lasing power duty cycle should provide a much better resolution in power density on the bone sample during our computer-controlled procedure when using beam with a larger diameter. Figure 5a shows how the temperature of a porcine bone sample is fluctuating within a 1ºC temperature range when it is positioned at 1.2 m from L_3. As beam profilometer usually have aperture that are smaller than 25mm, the beam spot size was calculated from a plot similar to the one shown in Figure 1b to be 90mm in diameter at 1.2 m from L_3. Note that the duty cycle of the lasing power has to alternate successively between 2.5% and 3% to keep the bone sample within the 1ºC margin as shown in Figure 5a.

Equations 7 and 8 were also used during heating and cooling as discussed in the mathematical modelling in section 3. Instead of reproducing all the percentage power in Figure 5a, from 6.5% to 3%, we have assumed a percentage power to change alternatively from 3% to 2.5% every second for 9 second in the mathematical model. The data for ρ, c, T_o, k and h were kept the same. As the experimental results in Figure 5a were obtained at a modulation frequency of 20 kHz, the simulation was also done at 20 kHz. As the beam spot size was calculated to be 90mm in Figure 5a, q_o was calculated to 70.7 W/m² and 59 W/m² at power percentages of 3% and 2.5%, respectively. The simulation described in section 3 is shown in Figure 5b for z=0. The simulation in Figure 5b shows that a larger temperature is reached, but the amplitude of the ripple in both the experimental data and the simulation are very comparable.

The higher temperature obtained from the simulation near the steady state is about 5°C greater that the experimental data, which is probably due to the radiative transfer loss that is not taken into account in the mathematical modelling. It was also assumed that the porcine bone absorbed all the optical energy delivered by the laser, which is not necessarily the case. Some optical energy that is scattered was not taken into account in the mathematical modelling. As a result, the temperature calculated is expected to be lower. Note that the power is fluctuating from 3% to 2.5% from 20s to 120s in Figure 5a. It is possible to notice in Figure 5a that the cycling period of the power percentage from 2.5% to 3% during feedback is sometimes more that 1s depending on sudden change in the convective transfer or minute change of the material properties such as specific heat c. The bone samples were also positioned at a distance of 1.75m from lens L_3, where the irradiance is significantly smaller as the beam spot size was calculated (c.f. Figure 1b) to be 139mm at that point.

The laser procedure was then repeated to keep the sample at a temperature around 40ºC. Note in Figure 5c that the percentage power must be increased to 9% for temperature to rise to 40ºC in order to compensate for the power density, which decreases with the distance from L_3. As the temperature is reaching the desired value of 40°C, it is fluctuating much less within 5s to 120s. In fact, the temperature variation is less than 1°C and remains within the two dash lines indicating 39°C and 40°C as shown in Figure 5c. In our simulation in

Figure 5d, we have kept the power percentage at 9% during the first 9 seconds and we can notice that the temperature rises to 45°C in a few seconds reaching a constant temperature of about 45°C without any ripples in the graph. For the simulation in Figure 5d, all data used to produce the graph in Figure 5b were kept the same, except q_o=22.2 W/m^2 at the specimen position. The temperature was calculated at z=0.

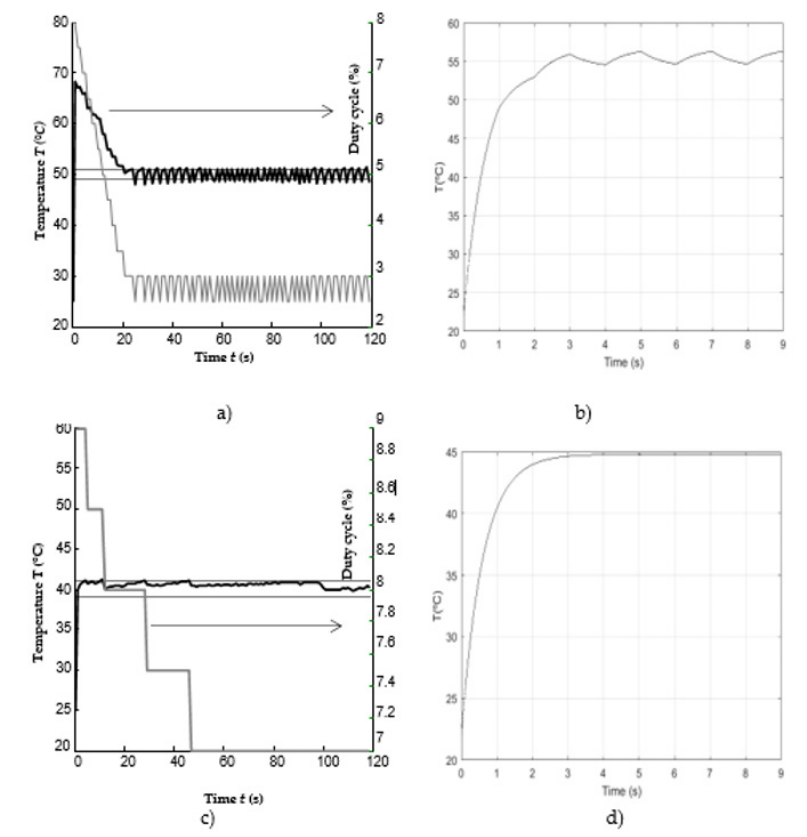

Figure 5:

a) Temperature as a function of time controlled at a modulation frequency of 20kHz. Temperature remains constant at 50°C within ±1°C from t= 20s to 120s. The power percentage (gray curve) can be read on the right hand side axis. The specimen position is 1.2m from L_3.

b) Simulation of the temperature for the power percentage shown in Figure 5a. Refer to the text for the data used to produce the curve.

c) Temperature as a function of time controlled at a modulation frequency of 20 kHz. Temperature remains constant at 40°C within less than 1°C from t= 5s to 120s. The power percentage (gray curve) can be read on the right hand side axis. The specimen position is 1.75m from L_3.

d) Simulation of the temperature for the power percentage shown in Figure 5c. Refer to the text for the data used to produce the curve.

Other insulators such as Teflon and glass can also be maintained at a steady temperature within 1°C. Teflon and glass have an absorption coefficient α of the order of 35 cm^{-1} and 600 cm^{-1}, respectively [30,31]. These absorption coefficients for the previously mentioned insulators are much less than that of bone, which is 2500 cm^{-1} as previously mentioned in section 3. Teflon and glass having a thickness of 1mm have been positioned in the collimated beam region at 1m from lens L_2, where the beam diameter is 10mm. As α is smaller, the density of power q_o must be higher to raise temperature in Teflon or glass. (Figure 6) shows the temperature in both Teflon and glass near 100°C for Teflon for a CO_2 laser delivering power at a frequency modulation of 20 kHz. Note that the power percentage required to maintain temperature at 100 ±1°C is larger for Teflon as α is smaller for Teflon compared to glass Figure 6.

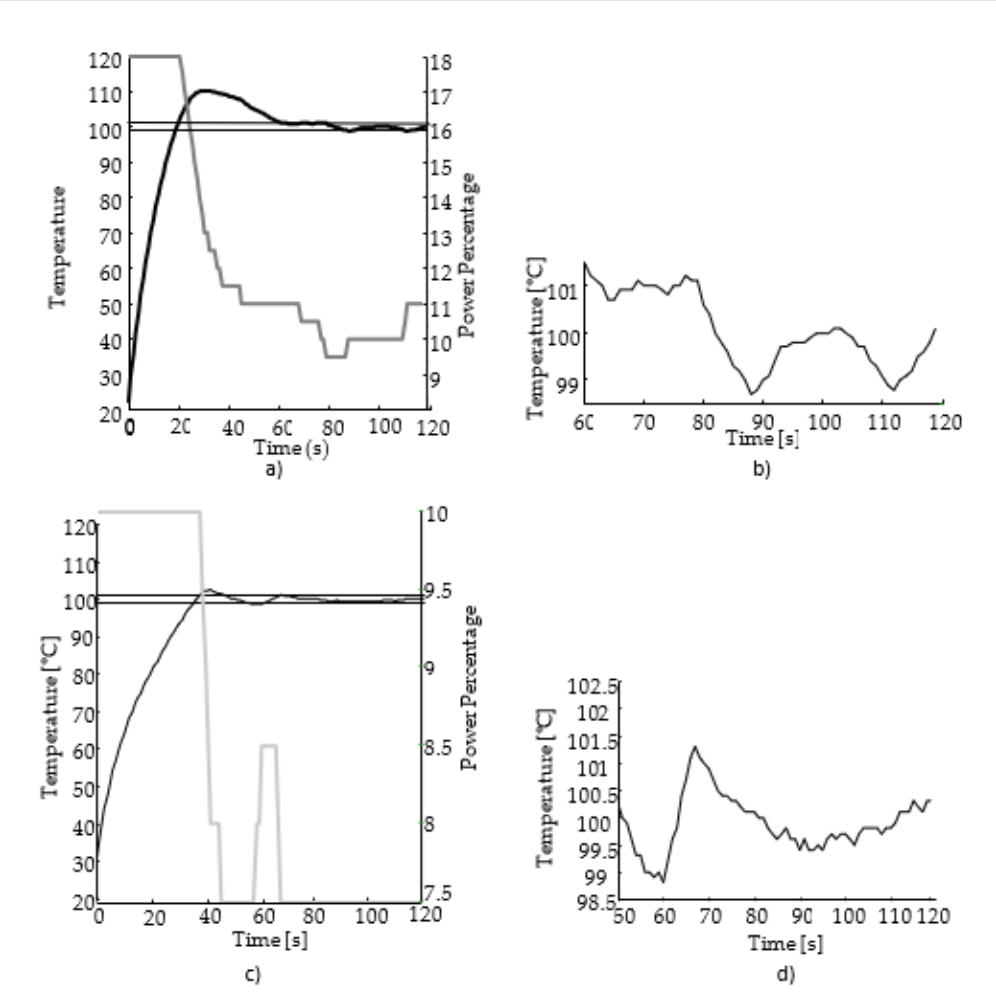

Figure 6:

a) Temperature (black curve) as a function of time in Teflon. The gray curve is showing the power percentage history during the control by feedback described in section 2.

b) Temperature variation from 60s to 120s when temperature reaches a nearly steady value around 100°C.

c) Temperature (black curve) as a function of time in glass. The curve in shaded gray is showing the power percentage history during the control by feedback described in section 2.

d) Temperature variation from 50s to 120s when temperature reaches a nearly steady value around 100°C.

Conclusion

It was shown that a CO_2 laser modulated at 20 kHz can be used to keep the temperature within 1°C in porcine bone, which corresponds to the thermal sensor uncertainty. It was also shown that the temperature of some insulators such as Teflon and glass can be maintained at temperatures within the uncertainty (±1°C) of the thermal sensor. A mathematical modelling was also proposed and it was shown that it describes very well the experimental data obtained.

References

1. S M Becker, A V Kuznetsov (2015) Heat transfer and fluid flow in biological processes. Elsevier.
2. F X Roux, L Merienne, B Leriche, S Lucerna, B Turak, et al. (1992) laser in Medical Sciences 7: 121-126.
3. Steven P A Parker, Arun A Darbar, John D B Featherstone, Giuseppe Iaria, Gabi Kesler, et al. (2007) The Use of Laser Energy for Therapeutic Ablation of Intraoral Hard Tissues. Journal of Laser Dentistry 15(2): 78-86.
4. Zhen Lin, Yi Liu, Xueming Ma, Shaoyu Hu, Jiawei Zhang, et al. (2015) Photothermal ablation of bone metastasis of breast cancer using PEGylated multi-walled carbon nanotubes. Sci rep 5: 11709.
5. Béla Hegedũs, Lászlo Viharos, Mihály Gervain, Márta Gálfi (2009) The Effect of Low-Level Laser in Knee Osteoarthritis: A Double-Blind, Randomized, Placebo-Controlled Trial. Phomed Laser Surg 27(4): 577-584.
6. Lars O Svaasand, Charles J Gomer, Elisa Morinelli (1990) On the Rationale of Laser induced Hyperthermia. Lasers in Medical Science 5: 121-128.

7. J S M Lai, C C Y Tham, D S C Lam (1999) Limited argon laser peripheral iridoplasty as immediate treatment for an acute attack of primary angle closure glaucoma: a preliminary study. Eye 13: 26-30.
8. JSM Lai, CCY Tham, JKH Chua, ASY Poon, JCH Chan, et al. (2006) To compare argon laser peripheral iridoplasty (ALPI) against systemic medications in treatment of acute primary angle-closure: mid-term results. Eye (20): 309-314.
9. H Deppe, HH Horch, A Neff (2007) Conventional versus CO2 laser-assisted treatment or peri- implant defects with concomitant use of pure-phase ß-tricalcium phosphate: A 5 year clinical report. Int J Oral Maxillofac Implants 22(1): 79-86.
10. L G Santos, J A Dominguez, A S Rebolledo, C G Escoda (2010) Thermal increment due to ErCr: YSGG and CO_2 laser irradiation of different implant surfaces. A pilot study. Med Oral Cir Bucal 15(5): 782-787.
11. Y Khan, M J Yaszemski, A G Mikos, C T Laurencin (2008) Tissue engineering of bone: material and matrix considerations. J Bone Joint Surg Am 90 (1): 36-42.
12. Luc Lévesque (2013) Temperature Control of Water-based Substances by CO2 laser for Medical Applications. Appl Opt 52(16): 3856-3863.
13. Luc Lévesque (2014) Law of Cooling, heat Conduction and Stefan-Boltzmann Radiation Laws fitted to Experimental Data for Bones irradiated by CO2 Laser. Biomedical Optics Express 5(3): 701-712.
14. Luc Lévesque (2015) Jean-Marc Noël and Calum Scott, Controlling the Temperature of Bones using pulsed CO_2 Lasers: Observations and Mathematical Modeling. Biomedical Optics Express 6(12): 4768-4780.
15. Luc Lévesque, Alek Robaczewski (2017) Very Accurate Temperature Control of Bones by CO2 Laser for Medical Applications. Appl Opt 56(13): 3923-3928.
16. Alexander Wainwright, Luc Lévesque (2021) Precise determination of the focal point on a glass sample using spectroscopic analysis. Appl Opt 60(12): 3535-3539.
17. M M Ivanenko, P Hering (1992) Wet bone ablation with mechanically Q-swithched high- repetition-rate CO_2 laser. Appl Phys B 67(3): 395-397.
18. A Sagi, A Shitzer, A Katzir, S Akselrod (1992) Heating of biological tissue by laser irradiation: theoretical model. Opt Eng 31(7): 1417-1424.
19. Foundation, www.itis.ethz.ch/itis-for-health/tissue-properties/database/density.
20. M M Ivanenko, P Hering (1998) Wet bone ablation with mechanically Q-swithched high- repetition-rate CO_2 laser. Appl Phys B 67(3): 395-397.
21. M Forrer, M Frenz, V Romano, H J Altermatt, H P Weber, et al. (1993) Bone Ablation mechanism Using CO_2 lasers of Different Pulse Duration and Wavelength. Appl Phys B 56(2): 104-112.
22. C E Webb, J C Jones (2004) Handbook of Laser Technology and Applications. Volume III: Applications, eds. (Institute of Physics Publishing), pp. 2067.
23. A N bashtakov, E A Genina, V I Kochubey, V V Tuckin (2006) Optical properties of human cranial bone in spectral range from 800 to 2000nm. Proc SPIE 6163: 616310.
24. J D B Featherstone, D Fried (2001) Fundamental interactions of lasers with dental and hard tissues. Med Laser Appl 16(3): 181-194.
25. D Fantarella, L Kotlow (2014) The 9.3 μm CO_2 dental laser: Technical development and early clinical experiences. J Laser Dent 22(1): 1.
26. G B Arfken, H J Weber, F E Harris (2005) Mathematical Methods for Physicists (6th Edn.)., Elsevier Academic, pp. 611-618.
27. E Butkov (1968) mathematical Physics (Addison-Wesley), pp. 296-299.
28. Y Yener, S Kakaç (2008) Heat Conduction (4th Edn.)., Taylor and Francis, pp. 210-212.
29. M N Özişik (1980) Heat Conduction. Wiley, pp. 276.
30. A Sagi, A Shitzer, A Katzir, S Akselrod (1992) Heating of biological tissue by laser irradiation: theoretical model. opt Eng 31(7): 1417-1424.
31. Foundation, www.itis.ethz.ch/itis-for-health/tissue-properties/database/density.

ISSN: 2574-1241

DOI: 10.26717/BJSTR.2023.48.007624

Luc Lévesque. Biomed J Sci & Tech Res